Accelerated Crystallization of Poly(L-lactide) by Physical Aging

Hideto Tsuji, Mariko Sawada

Department of Ecological Engineering, Faculty of Engineering, Toyohashi University of Technology, Tempaku-cho, Toyohashi, Aichi 441-8580, Japan

ABSTRACT: The low-temperature physical aging of amorphous poly(L-lactide) (PLLA) at 25–50°C below glass transition temperature (T_g) was carried out for 90 days. The physical aging significantly increased the T_g and glass transition enthalpy, but did not cause crystallization, regardless of aging temperature. The nonisothermal crystallization of PLLA during heating was accelerated only by physical aging at 50°C. These results indicate that the structure formed by physical aging only at 50°C induced the accelerated crystallization of PLLA during heating, whereas the structure formed by physical aging at 25 and 37°C had a negligible effect on the crystallization of PLLA during heating, except when the physical aging at 37°C was continued for the period as long as 90 days. The mechanism for the accelerated crystallization of PLLA by physical aging is discussed. © 2009 Wiley Periodicals, Inc. J Appl Polym Sci 116: 1190–1196, 2010

Key words: aging; crystallization; nucleation; poly(L-lactic acid); structure

INTRODUCTION

Enhancement of heat resistance or thermal stability of biomass-derived poly(L-lactide), that is, poly(L-lactic acid) (PLLA) (Scheme 1), is a matter of concern when PLLA is utilized for various purposes, including industrial and commodity applications.[1–14] Elevating crystallinity is effective for increasing the thermal dimensional stability. The addition of nucleating agents is one of the most commercially advantageous methods for increasing the crystallinity in a limited period of processing. Reported biodegradable nucleating agents for PLLA are poly(glycolide)[15,16] and stereocomplex of PLLA/poly(D-lactide), that is, poly(D-lactic acid) (PDLA).[17–21]

Meanwhile, low-temperature physical aging below glass transition temperature (T_g) was found to induce the brittle nature of PLLA.[22] Very recently, Pan et al. investigated the effects of physical aging at 40 and 50°C for the period up to 35 days on mechanical properties and isothermal crystallization.[23]

In a previous study, the melt-quenching was found to enhance the self-nucleating of PLLA and, therefore, increases the number of spherulites per unit area, resulting in the rapid completion of isothermal crystallization.[24]

Yu et al. and Martino et al. investigated the effect of physical aging at 50°C and 28°C, respectively, on the nonisothermal crystallization of PLLA in contact with compressed carbon dioxide and in the presence of polyadipates.[25,26] Although the enhanced crystallization of PLLA was observed in contact with the carbon dioxide at a pressure of 2 atm and in the presence of polyadipates, no significant effect was noticed for the blank tests at relatively high temperature of 50°C in a short period of 6.25 days or at a relatively low-temperature of 28°C even after a long period of 150 days. On the other hand, Mohamed et al. investigated the effect of physical aging at room temperature on the nonisothermal crystallization of PLLA as the blank tests of PLLA/cuphea or lesquerella composites for 30 days.[27] However, no significant effect on the nonisothermal crystallization of PLLA was observed. As far as we are aware, the effect of physical aging on the nonisothermal crystallization of PLLA has not been investigated in detail for a wide temperature range below T_g and for a long period. Considering the low-temperature physical aging, the reported data for the nonisothermal crystallization of melt-quenched PLLA with various additives during heating[15,16,21,28,29] might be affected by the storage period at room temperature (25°C).
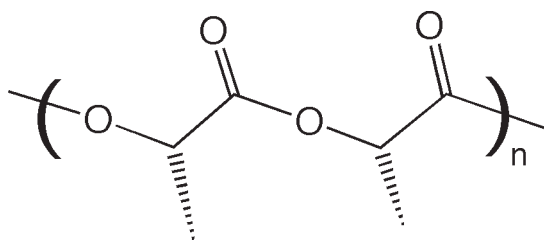
Scheme 1 Molecular structure of PLLA.

The purpose of the present study was to investigate in detail the effects of physical aging on the nonisothermal crystallization of PLLA. For this purpose, we have carried out physical aging of amorphous PLLA in a wide temperature range of 25–50°C below T_g for a long period up to 90 days, investigated the effects of physical aging on the nonisothermal crystallization of amorphous PLLA during heating by differential scanning calorimetry (DSC), and the crystallization kinetics was estimated by the use of Avrami theory.

EXPERIMENTAL

Materials

PLLA [intrinsic viscosity = 5.7–8.2, number-average molecular weights (M_n) = 5.7 × 10^5 g mol^{-1}, polydispersity index = 2.0] was purchased from Polysciences (Warrington, PA) and purified by precipitation using chloroform as the solvent and methanol as the nonsolvent. The purified PLLA was dried under reduced pressure for more than one week. The PLLA films having a thickness of 50 μm were prepared by a solution-casting method using dichloromethane as the solvent. The obtained films were dried under reduced pressure for at least 7 days. The amorphous PLLA films were prepared by

the following procedure.[21,24] Each of dried PLLA films was placed between two Teflon sheets and sealed in a glass tube under reduced pressure. After the sealing, the PLLA films were melted at 200°C for 5 min and quenched into iced water (0°C). Each of the amorphous PLLA films was physically aged in the sealed state at 25, 37, and 50°C for up to 90 days (2160 hours).

Measurements and observation

The thermal properties and crystallization behavior of the physically aged PLLA films were monitored during heating using a Shimadzu (Kyoto, Japan) DSC-50 differential scanning calorimeter under nitrogen gas flow at a rate of 50 mL min^{-1}. For DSC measurements, the physically aged PLLA films were heated at a rate of 10°C min^{-1} from room temperature to 200°C. The temperatures of glass transition, cold crystallization, and melting (T_g, T_{cc}, and T_m, respectively) and the enthalpies of glass transition, cold crystallization, and melting (ΔH_g, ΔH_{cc}, and ΔH_m, respectively) were calibrated using benzophenone, indium, and tin as the standards. We have measured triplicate samples for each data point. The weight-average molecular weight (M_w) and M_n of PLLA were evaluated in chloroform at 40°C with a Tosoh (Tokyo, Japan) GPC system having two TSK gel columns (GMH$_{XL}$) using polystyrene standards.

RESULTS AND DISCUSSION

In the present study, the physical aging temperatures (25, 37, and 50°C) were selected to be lower than T_g (60°C) to ensure the significant physical aging effect on glass transition behavior and to avoid the crystallization of PLLA.[22,23,25–27,30,31] There
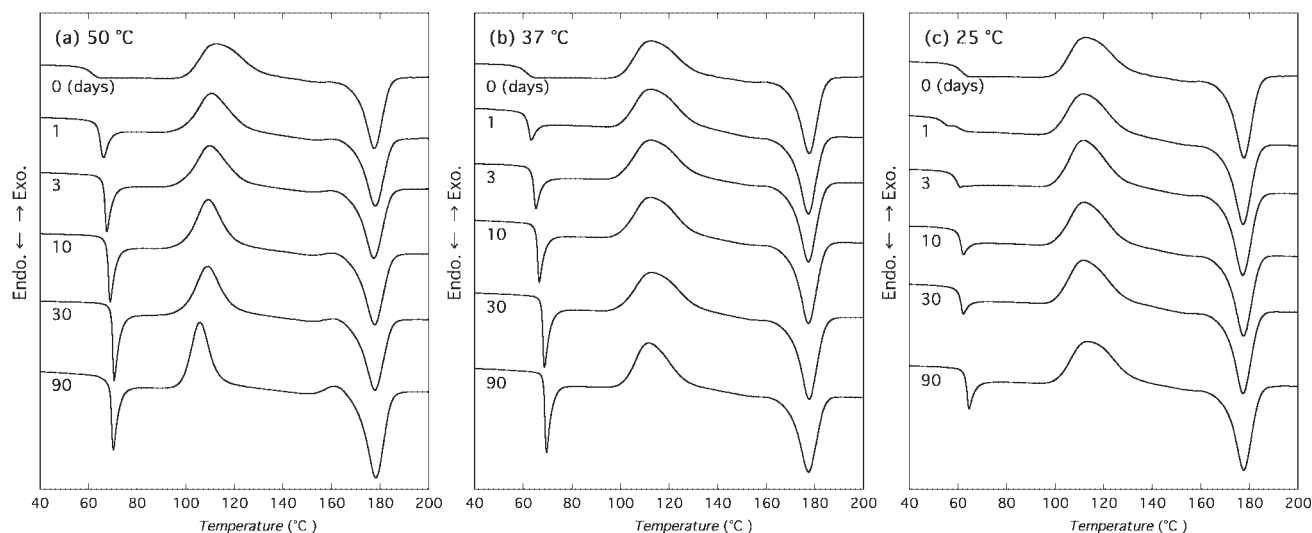

Figure 1 DSC thermograms of melt-quenched PLLA after physical aging at 50°C (a), 37°C (b), and 25°C (c).
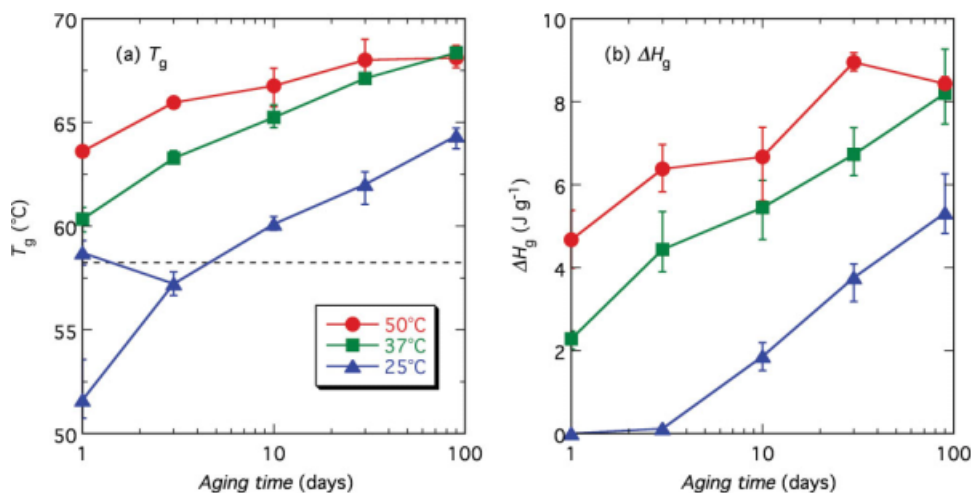
Figure 2 Glass transition temperature (a) and enthalpy (b) (T_g and ΔH_g, respectively) of melt-quenched PLLA after physical aging at different temperatures. The broken line shows the initial T_g value at 0 day. The initial ΔH_g value at 0 day was nil. [Color figure can be viewed in the online issue, which is available at www.interscience.wiley.com.]

is an optimal physical aging temperature with the highest effect on glass transition behavior.[30,31] The aging temperature of 50°C was selected to be just below T_g. The aging temperature of 37°C is the human body temperature. The obtained data at this temperature should be useful as blank data for *in vivo* biomedical applications of PLLA. On the other hand, the aging temperature of 25°C was selected to be lower than T_∞ (T_g−30°C) where all motion associated with viscous flow ceases and the preformed PLLA articles are often expected to be stored.

Figure 1 shows the DSC thermograms of PLLA physically aged at different temperatures and times. The glass transition, cold crystallization, and melting peaks were observed at 60°C, 100–150°C, and 160–170°C, respectively. The T_g, onset, peak, and endset temperatures of cold crystallization [$T_{cc}(O)$, $T_{cc}(P)$, and $T_{cc}(E)$, respectively], ΔH_g, ΔH_{cc}, and ΔH_m were

estimated from Figure 1. The procedures for estimating T_{cc} values were reported elsewhere, although in the literature onset and endset temperatures are expressed as starting and ending temperature, respectively.[28,29] The obtained data are plotted as a function of aging time in Figures 2 and 3 and those at 0 and 90 days are summarized in Table I. The two T_g data at one day (25°C) means the multiple glass transition, although we don't know the cause for it.

The T_g and ΔH_g values increased with aging time (Fig. 2), reflecting the amorphous chains took more stable comformational structure and were packed densely, irrespective of physical aging temperature. This trend is consistent with the results reported by Cai et al. and Pan et al.[22,23,31] The initial increase rate of T_g and ΔH_g became higher with an increase in aging temperature. It is interesting to note that the physical aging for only one day has significant
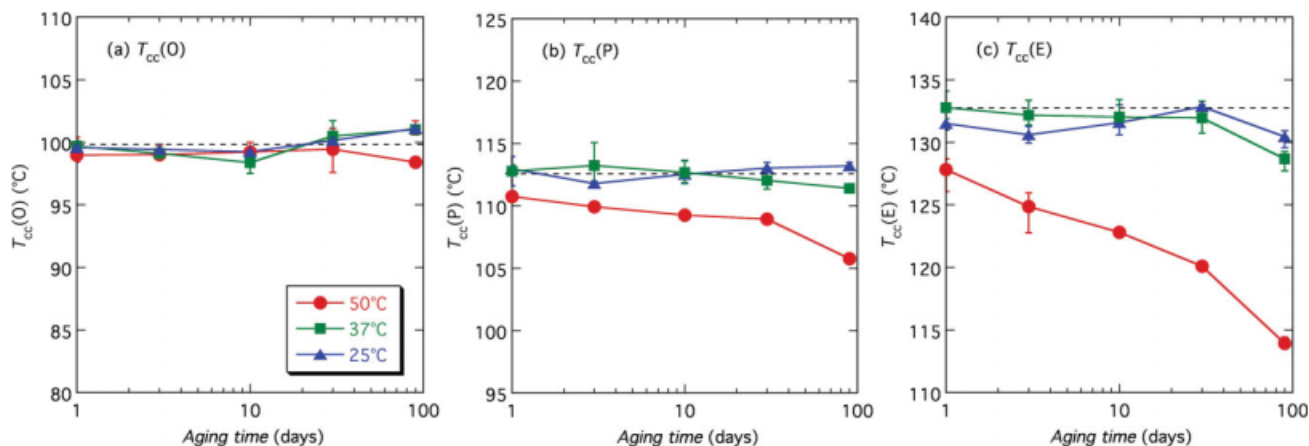

Figure 3 $T_{cc}(O)$ (a), $T_{cc}(P)$ (b), and $T_{cc}(E)$ (c) of melt-quenched PLLA after physical aging at different temperatures as a function of aging time. The broken lines show the initial values at 0 day. [Color figure can be viewed in the online issue, which is available at www.interscience.wiley.com.]

TABLE I
Thermal Properties of Melt-Quenched PLLA Before and After Physical Aging for 90 Days

Aging conditions		T_g[a]	$T_{cc}(O)$[a]	$T_{cc}(P)$[a]	$T_{cc}(E)$[a]	T_m[a]	ΔH_g[b]	ΔH_{cc}[b]	ΔH_m[b]
Temperature (°C)	Time (days)	(°C)	(°C)	(°C)	(°C)	(°C)	(J g^{-1})	(J g^{-1})	(J g^{-1})
–	0	58.1	99.5	112.7	132.4	177.4	0	31.7	33.9
25	90	64.4	101.1	113.2	130.5	177.4	5.3	32.2	33.7
37	90	68.4	101.0	111.4	128.7	177.4	8.2	32.5	33.0
50	90	68.1	98.4	105.8	113.9	178.0	8.4	30.4	32.9

[a] T_g, $T_{cc}(O)$, $T_{cc}(P)$, and $T_{cc}(E)$ are glass transition temperature, starting, peak, and ending temperatures of cold crystallization, respectively.
[b] ΔH_g, ΔH_{cc}, and ΔH_m are glass transition, cold crystallization and melting enthalpies, respectively.

effects on T_g and ΔH_g values. As seen in Figure 3, at aging temperatures of 25 and 37°C the $T_{cc}(O)$, $T_{cc}(P)$, and $T_{cc}(E)$ values, excluding the significant decrease of $T_{cc}(E)$ at 90 days (37°C), were practically constant throughout the period studied here. This finding and the unchanged ΔH_{cc} and ΔH_m values after physical aging (Table I) strongly suggest that the physical aging at 25 and 37°C has no significant or a negligible effect on the cold crystallization behavior of PLLA. This result means that the reported cold crystallization data was not affected by the storage (i.e., physical aging) below T_g, such as at around room temperature (25°C), at least for up to 90 days after thermal treatment such as melting at the temperature exceeding T_g.[15,16,21,28,29] On the other hand, at aging temperature of 50°C, $T_{cc}(P)$ and $T_{cc}(E)$ values significantly decreased but the $T_{cc}(O)$, ΔH_{cc}, and ΔH_m values remained unchanged for all the periods (Fig. 3 and Table I). This finding indicates that only the structure formed by physical aging at 50°C could accelerate the cold crystallization of PLLA after the onset of crystallization. The $T_{cc}(O)$ values are varied by the accelerated or disturbed nucleating effect, whereas the $T_{cc}(P)$ and $T_{cc}(E)$ values are altered by

the $T_{cc}(O)$ and spherulite (crystallite) number per unit mass during crystallization. Therefore, no significant change of $T_{cc}(O)$ and the significant decreases of $T_{cc}(P)$ and $T_{cc}(E)$ values during physical aging indicate the increased number of spherulite (crystallite) per unit mass, as reported by Pan et al. for isothermal crystallization.[23]

To elucidate the relationship between $T_{cc}(E)$ and T_g or ΔH_g, the $T_{cc}(E)$ values were plotted in Figure 4 as functions of T_g and ΔH_g. Here, $T_{cc}(O)$ and $T_{cc}(P)$ were not used for plot, because they were altered insignificantly or to a very small extent by the physical aging. At 50°C, the $T_{cc}(E)$ values decreased with increases in T_g and ΔH_g, whereas at 25 and 37°C, the $T_{cc}(E)$ values were practically constant, excluding the $T_{cc}(E)$ values at T_g above 68°C and at ΔH_g above 8 J g^{-1}. This again is indicative of the fact that the structures formed at 25 and 37°C, excluding that with T_g above 68°C and at ΔH_g above 8 J g^{-1}, had no significant effect on the cold crystallization of PLLA, despite of the significant increases in T_g and ΔH_g values during physical aging. On the other hand, only the structure formed at 50°C, which was also accompanied by the significant increases in T_g
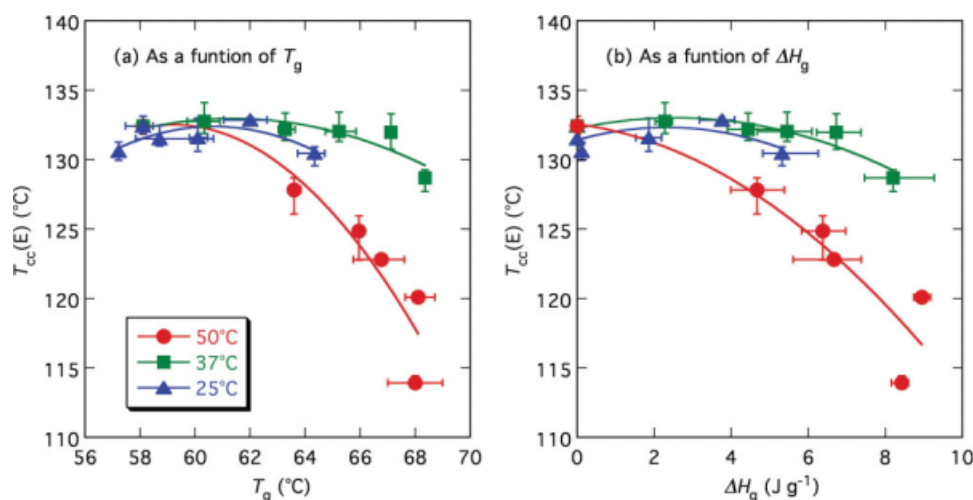

Figure 4 $T_{cc}(E)$ of melt-quenched PLLA after physical aging at different temperatures as functions of T_g (a) and ΔH_g (b). [Color figure can be viewed in the online issue, which is available at www.interscience.wiley.com.]
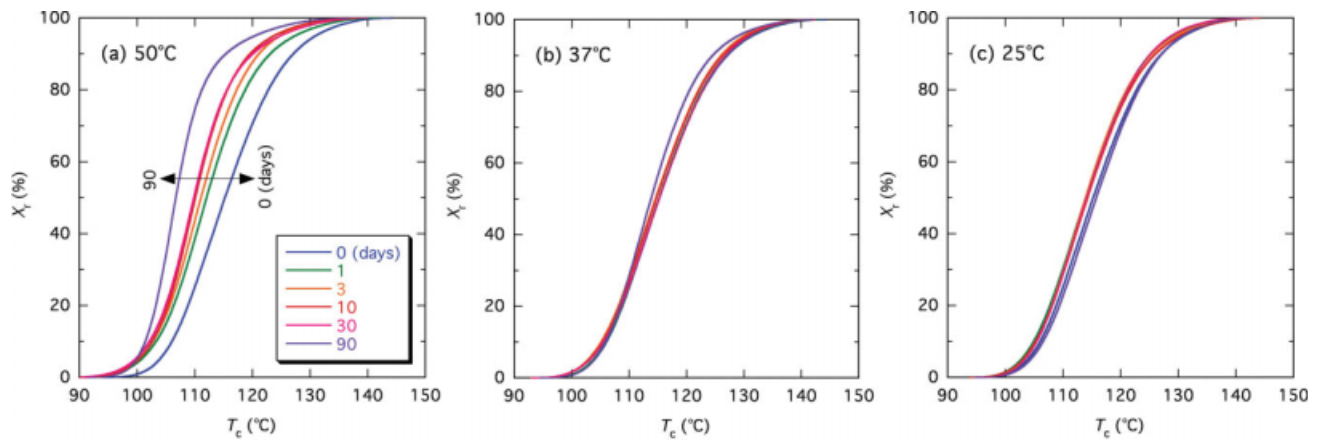
Figure 5 Relative crystallinity (X_r) of melt-quenched PLLA physically aged at 25°C (a), 37°C (b), and 50°C (c) as a function of crystallization temperature (T_c) during heating DSC heating. [Color figure can be viewed in the online issue, which is available at www.interscience.wiley.com.]

and ΔH_g values as in the physical aging at 25 and 37°C, can accelerate the cold crystallization during heating.

The crystallinity relative to that after the completion of cold crystallization during heating from the room temperature (X_r) of PLLA was obtained from Figure 1 and is plotted in Figure 5 as a function of crystallization temperature (T_c) during DSC heating. The X_r is defined as follows:

$$X_r = 100 \int_0^t (dH_{cc}/dt)dt / \int_0^\infty (dH_{cc}/dt)dt \quad (1)$$

where dH_{cc} denotes the measured enthalpy of cold crystallization during an infinitesimal time interval dt. Crystallization kinetics was analyzed from DSC data by the use of the Avrami theory,[32–34] which is expressed by the following equation, assuming that the primary stage of nonisothermal crystallization can be described by the Avrami equation, as suggested by Mandelkern:[35]

$$1 - X_r/100 = \exp(-k_r t_c^{\,n}) \quad (2)$$

where X_r is expressed in %, k_r is the nonisothermal crystallization rate constant, n is the Avrami exponent, and t_c is the crystallization time defined by the following equation:

$$t_c = (T_c - T_0)/\Phi \quad (3)$$

where T_0 is the T_c where crystallization starts and Φ (K min^{-1}) is heating rate. In the present study, T_0 was assumed to be 90°C. Equation (2) can be transformed to eq. (4).

$$\ln[-\ln(1 - X_t/100)] = \ln k_r + n \ln t_c \quad (4)$$

To avoid the deviation from the theoretical curves, as stated by Mandelkern[34] at X_r exceeding 25%, and the effect of relatively low S/N ratio in the initial stage at X_r below 5%, we used X_r in the range of 5–25% for estimating n and k_r. Figure 6 shows the plots
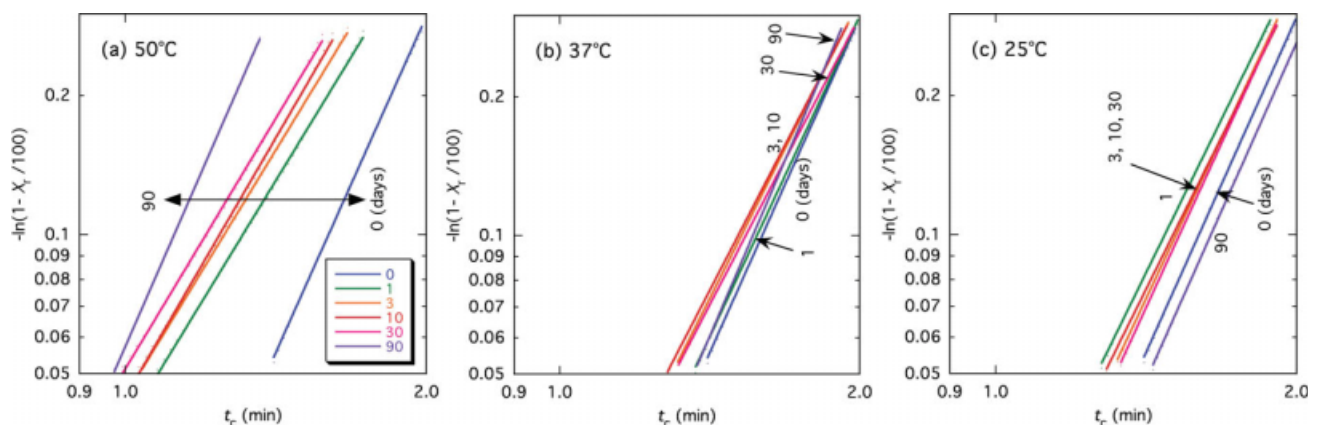

Figure 6   -ln (1- X_r/100) of melt-quenched PLLA physically aged at 25°C (a), 37°C (b), and 50°C (c) as a function of crystallization time (t_c) during DSC heating. [Color figure can be viewed in the online issue, which is available at www.interscience.wiley.com.]

Avrami Exponent (n), Crystallization Rate Constant (k_r and k), and Half-Time ($t_{1/2}$) for Nonisothermal and Isothermal Crystallization of PLLA Physically Aged with Different Conditions

| Aging conditions | | | | | k_r | k | $t_{1/2}$ (min) | |
Temperature (°C)	Time (days)	T_c range for estimation (°C)	Average T_c (°C)	n	(Nonisothermal crystallization)	(Isothermal crystallization)	Nonisothermal crystallization	Isothermal crystallization
–	0	104.1–110.0	107.1	4.82	0.0104	0.634	2.39	1.02
25	1	102.8–108.8	105.8	4.40	0.0180	0.669	2.29	1.01
	3	103.2–109.1	106.2	4.60	0.0148	0.656	2.31	1.01
	10	102.9–109.1	105.6	4.36	0.0168	0.665	2.35	1.01
	30	103.3–109.1	106.2	4.70	0.0136	0.651	2.31	1.01
	90	104.4–110.4	107.4	4.85	0.0090	0.624	2.45	1.02
37	1	103.7–109.9	106.8	4.63	0.0121	0.643	2.40	1.02
	3	103.1–109.5	106.3	4.30	0.0164	0.663	2.39	1.01
	10	102.8–109.4	106.1	4.17	0.0179	0.669	2.40	1.01
	30	103.2–109.7	106.5	4.16	0.0167	0.664	2.45	1.01
	90	103.8–109.2	106.5	5.05	0.0105	0.634	2.29	1.02
50	1	100.8–107.5	104.2	3.55	0.0382	0.722	2.26	0.99
	3	100.4–106.7	103.6	3.55	0.0445	0.733	2.17	0.98
	10	100.3–106.3	103.3	3.72	0.0445	0.733	2.09	0.99
	30	100.0–106.0	103.0	3.60	0.0512	0.743	2.06	0.98
	90	99.8–103.9	101.9	4.95	0.0573	0.745	1.66	0.98

with eq. (4) of PLLA physically aged at different temperatures. These plots give n as a slope and the intercept ln k_r. The k_r values for nonisothermal crystallization should be corrected to the k values for isothermal crystallization by eq. (5), as suggested by Jeziorny:[36]

$$\ln\ k = (\ln\ k_r)/\Phi \qquad (5)$$

Also, the half-time ($t_{1/2}$) for the cold crystallization of PLLA was calculated by the following equation:

$$t_{1/2} = [(\ln\ 2)/k]^{1/n} \qquad (6)$$

Obtained n, k_r, k, and $t_{1/2}$ for nonisothermal and isothermal crystallization are tabulated in Table II. The estimated Avrami exponent n values were in the range from 3.6 to 5.1. These values are comparable with four reported by Miyata and Masuko[37] but slightly higher than three reported by Tsuji et al.[21] The average n value from 1 to 30 days was lower for 50°C than for 25 and 37°C, suggesting the difference between the crystallite growth dimensions at 50°C and at 25 and 37°C. On the other hand, the k_r (k) and $t_{1/2}$ values at 50°C were respectively higher and shorter than those at 25 and 37°C. This confirms that the crystallization rate was elevated by the physical aging at 50°C. The difference in $t_{1/2}$ values between 25 and 37 and 50°C were small for isothermal crystallization. In addition to the correction of k value by eq. (6), this should be partly due to the difference in T_c range for estimation of k and $t_{1/2}$ values. That is, the k value obtained for rapid crystallization which took place at low T_c range is underestimated compared to that for slow crystallization which occurred at high T_c range, because normally crystallization

rate increases with T_c as far as T_c is below 130°C. This can cause the small difference in $t_{1/2}$ values.

The results obtained in the present study indicated that the cold crystallization of PLLA was accelerated by low-temperature physical aging at 50°C. This effect was observed at 37°C only when the aging was continued for the period as long as 90 days. To clarify whether or not the crystallization of PLLA
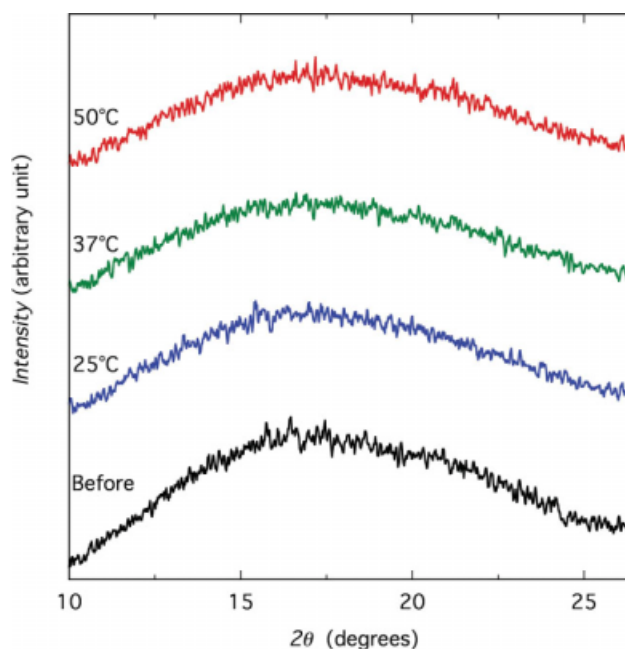

Figure 7 Wide-angle X-ray diffraction profiles of PLLA before physical aging and after physical aging at shown different temperatures for 90 days. [Color figure can be viewed in the online issue, which is available at www.interscience.wiley.com.]

during physical aging took place, wide-angle X-ray scattering measurements were carried out for the PLLA films physically aged at different temperatures for 90 days. However, as seen in Figure 7, no crystalline peaks were discerned in these specimens, indicating that these films were completely amorphous during physical aging. This is in contrast with the blocky copolymers of L-lactide and ε-caprolactone, which crystallization take place even at 25 and 37°C.[38–40] Therefore, the most probable explanation for such accelerated crystallization should be as follows. The mesomorphic phase (the intermediate inhomogeneous phase between crystalline phase and homogeneous amorphous phase) as reported by Konishi et al. should be formed in the PLLA physically aged at 50°C and facilitates the formation of crystallite nuclei,[41] resulting in the rapid crystallization during DSC heating in the present study. Such mesomorphic structure formation may be the conformational rearrangement from gg to gt to some extent[23] and conformational change is expected to be remarkable for the aging at a higher temperature as far as it is lower than T_g. However, the change in the fraction of gt relative to that of gg could not be traced by Fourier transform infrared (FTIR) spectroscopy, probably because the fractional change was very low. Such assignment has been reported for syndiotactic polystyrene in the induction period from FTIR data.[42] Further detailed study is required to elucidate the mechanism of accelerated crystallization of physically aged PLLA.

CONCLUSIONS

The physical aging of amorphous-made PLLA below T_g increased the T_g and ΔH_g, but did not induce the crystallization. The structure formed only at the highest aging temperature (50°C) can accelerate the cold crystallization of PLLA after the onset of crystallization.

References

1. Kharas, G. B.; Sanchez-Riera, F.; Severson, D. K. Plastics from Microbes; Mobley, D. P., Eds.; Hanser Publishers: New York, 1994; pp 93–137.
2. Doi, Y.; Fukuda, K., Eds. Studies in Polymer Science: Biodegradable Plastics and Polymers; Elsevier: Amsterdam, 1994; Vol. 12.
3. Li, S.; Vert, M. Degradable Polymers. Principles and Applications; Scott, G.; Gilead, D., Eds.; Chapman and Hall: London, 1995; pp 43–87.
4. Hartmann, M. H. Biopolymers from Renewable Resources; Kaplan, D. L., Ed.; Springer: Berlin, 1998; pp 367–411.
5. Ikada, Y.; Tsuji, H. Macromol Rapid Commun 2000, 21, 117.
6. Garlotta, D. J Polym Environ 2001, 9, 63.
7. Albertsson, A.-C., Ed. Advances in Polymer Science. Degradable Aliphatic Polyesters; Springer: Berlin, 2002; Vol. 157.
8. Södergård, A.; Stolt, M. Pro Polym Sci 2002, 27, 1123.
9. Scott, G., Ed. Biodegradable Polymers: Principles and Applications, 2nd ed.; Kluwer Academic Publishers: Dordrecht, 2002.
10. Tsuji, H. Biopolymers; Doi, Y.; Steinbüchel, A., Eds.; Wiley-VCH: Weinheim, 2002; Vol. 4, pp 129–177.
11. Auras, R.; Harte, B.; Selke, S. Macromol Biosci 2004, 4, 835.
12. Slager, J.; Domb, A. J. Adv Drug Delivery Rev 2003, 55, 549.
13. Tsuji, H. Macromol Biosci 2005, 5, 569.
14. Gupta, A. P.; Kumar, V. Eur Polym J 2007, 43, 4053.
15. Tsuji, H.; Tashiro, K.; Bouapao, L.; Narita, J. Macromol Mater Eng 2008, 293, 947.
16. Tsuji, H.; Sawada, M; Bouapao, L. ACS Appl Mater Interfaces 2009, 1, 1719–1730.
17. Brochu, S.; Prud'homme, R. E.; Barakat, I.; Jérôme, R. Macromolecules 1995, 28, 5230.
18. Schmidt, S. C.; Hillmyer, M. A. J Polym Sci Part B: Polym Phys 2001, 39, 300.
19. Yamane, H.; Sasai, K. Polymer 2003, 44, 2569.
20. Anderson, K. S.; Hillmyer, M. A. Polymer 2006, 47, 2030.
21. Tsuji, H.; Takai, H.; Saha, S. K. Polymer 2006, 47, 3826.
22. Pan, P.; Zhu, B.; Inoue, Y. Macromolecules 2007, 40, 9664.
23. Pan, P.; Liang, Z.; Zhu, B.; Dong, T.; Inoue, Y. Macromolecules 2008, 41, 8011.
24. Tsuji, H.; Ikada, Y. Polymer 1995, 36, 2709.
25. Yu, L.; Liu, H.; Dean, K. Polym Int 2009, 58, 368.
26. Martino, V. P.; Ruseckaite, R. A.; Jiménez, A. Polym Int 2009, 58, 437.
27. Mohamed, A.; Finkenstadt, V. L.; Rayas-Duarte, P.; Debra E, P.; Gordon, S. H. J Appl Polym Sci 2009, 111, 114.
28. Tsuji, H.; Kawashima, Y.; Takikawa, H.; Tanaka, S. Polymer 2007, 48, 4213.
29. Tsuji, H.; Kawashima, Y.; Takikawa, H. J Polym Sci Part B: Polym Phys 2007, 45, 2167.
30. Monstserrat, S. J Polym Sci Part B: Polym Phys 1994, 32, 509.
31. Cai, H.; Dave, V.; Gross, R. A.; Mccarthy, S. P. J Polym Sci Part B: Polym Phys 1996, 34, 2701.
32. Avrami, M. J Chem Phys 1939, 7, 1103.
33. Avrami, M. J Chem Phys 1940, 8, 212.
34. Avrami, M. J Chem Phys 1941, 9, 177.
35. Mandelkern, L. Crystallization of Polymers; McGraw-Hill: New York, 1964.
36. Jeziorny, A. Polymer 1978, 19, 1142.
37. Miyata, T.; Masuko, T. Polymer 1998, 39, 5515.
38. Tsuji, H.; Mizuno, A.; Ikada, Y. J Appl Polym Sci 2000, 76, 947.
39. Saha, S. K.; Tsuji, H. React Funct Polym 2006, 66, 1362.
40. Saha, S. K.; Tsuji, H. J Appl Polym Sci 2009, 112, 715.
41. Konishi, T.; Nishida, K.; Kanaya, T. Macromolecules 2006, 39, 8035.
42. Matsuba, G.; Kaji, K.; Nishida, K.; Kanaya, T.; Imai, M. Macromolecules 1999, 32, 8932.